ISSN 0967-859X
THE SOCIETY FOR EARTHQUAKE AND CIVIL ENGINEERING DYNAMICS

# NEWSLETTER

Volume 25 No 2
April 2014

## In this issue



# Forensic Seismology

**Ross Heyburn**
*AWE Blacknest*
*Brimpton, Reading*

Forensic seismology is the application of seismological methods to the detection, identification and characterisation of the seismic signals generated by nuclear test explosions. The home of forensic seismology in the UK is at AWE Blacknest, where a group of scientists provide the UK government with advice on monitoring nuclear test explosions. For example, the group recently analysed seismic signals from the 12th February 2013 announced North Korea nuclear test explosion to detect, locate, identify and estimate the yield of the explosion.

Forensic seismology originated during the Cold War. Various countries were beginning to develop and test nuclear weapons and it was soon realised that seismological methods provided a powerful means of monitoring this testing, particularly as the seismic signals could often be detected thousands of kilometres from the locations of the explosions. One of the major challenges in forensic seismology is discriminating between the seismic signals generated by earthquakes and those generated by explosions. The group in the UK at AWE was set up in the late 1950s and began developing the techniques required to do this.

Scientific development in the UK in Forensic Seismology has often been driven by international treaties that have been negotiated to control nuclear weapons testing. In 1996, the Comprehensive Nuclear-Test-Ban Treaty (CTBT) was opened for signature. Signatories undertake not to conduct nuclear weapons tests on their own territories, or encourage or participate in any nuclear test explosion in another territory. The ability to detect and identify nuclear test explosions wherever they might occur in the world, whether that is underground, in the oceans or in the atmosphere is therefore important for verifying compliance with the CTBT. To do this, seismologists in the UK at AWE Blacknest use data from the International Monitoring System (IMS), a global network of sensors established by

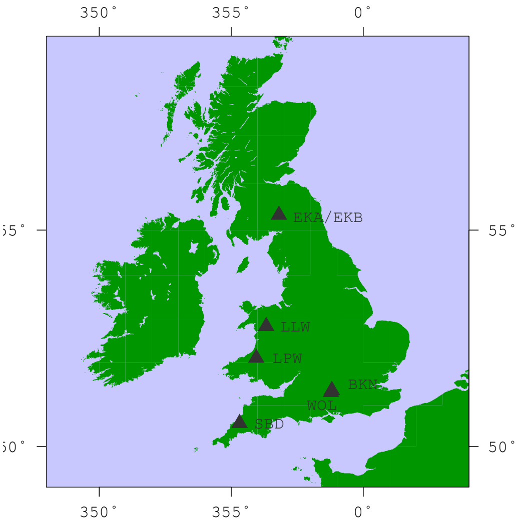


**Figure 1: Location of seismometer stations operated by AWE Blacknest in the UK.**

the CTBT organisation to remotely detect nuclear test explosions. As well as seismic stations, the IMS consists of a network of hydroacoustic, infrasound and radionuclide stations. The UK operates a seismometer array at Eskdalemuir and a radionuclide laboratory, both of which contribute data to the IMS. Data from the IMS are transmitted to the International Data Center (IDC) in Vienna and here event bulletins are compiled. Countries which have signed the CTBT have access to data from the IMS along with the event bulletins and these are used for monitoring nuclear test explosions.

The primary task of the forensic seismology programme in the UK is the ability to provide the UK government with detailed analyses of seismic disturbances of special interest. These can for example include announced nuclear test explosions or seismic disturbances near to known nuclear test sites. To support this capability the group has a research program which develops the methodologies required to do this. Recent research carried out at AWE Blacknest has included developing improved methods of locating seismic and acoustic sources (e.g., Nippress et al., 2014), improving signal detection at seismometer arrays (Selby, 2013), and developing improved methods of seismic source depth estimation (Heyburn et al., 2013).

The group also operate a network of seismic and infrasound stations in the UK (Figure 1) to complement the data available to the group from the IMS. The principal station in the network is a seismometer array at Eskdalemuir in southern Scotland. This station consists of 20 individual seismometers spread along two lines each around 10 km in length. The advantages of seismometer arrays such as Eskdalemuir are that they allow an approximate source location to be estimated from a single station, and various different signal processing methods can be used to enhance seismic signals in the noise, thus ensuring lower amplitude signals can be detected than at single channel stations. Seismologists in the group are also responsible for advising the UK government on technical matters relating to monitoring the CTBT using the IMS. This type of work often involves evaluating the IMS data and event bulletins produced by the IDC in Vienna.

## Discriminating Between Earthquake and Explosion Sources

Forensic seismologists use a variety of methods to discriminate between the seismic signals generated by naturally occurring seismic sources such as earthquakes, and those generated by nuclear test explosions. It should however be noted that seismology and the other waveform verification technologies that are part of the IMS cannot be used to discriminate between nuclear explosions and other types of explosion. The only way to confirm that an explosion identified by the waveform verification is nuclear is to use data from the IMS radionuclide stations.

### The $m_b$ and $M_s$ Method

One of the most commonly used methods to identify earthquake sources, is to compare the ratio of the body-wave to surface wave magnitude, $m_b$:$M_S$. This is because it has often been observed that underground nuclear test explosions have smaller amplitude surface waves than an earthquake with the same body wave magnitude (Liebermann and Pomeroy, 1967). Figure 2 shows an example of seismograms recorded for an earthquake and explosion in China. The first arriving waves on both seismograms are the body (*P*) waves and the later arriving long-period waves are a type of surface wave known as Rayleigh waves. The Rayleigh waves are however of much smaller amplitude for the explosion than for the earthquake. This type of discrimination is applied formally using body and surface wave magnitudes

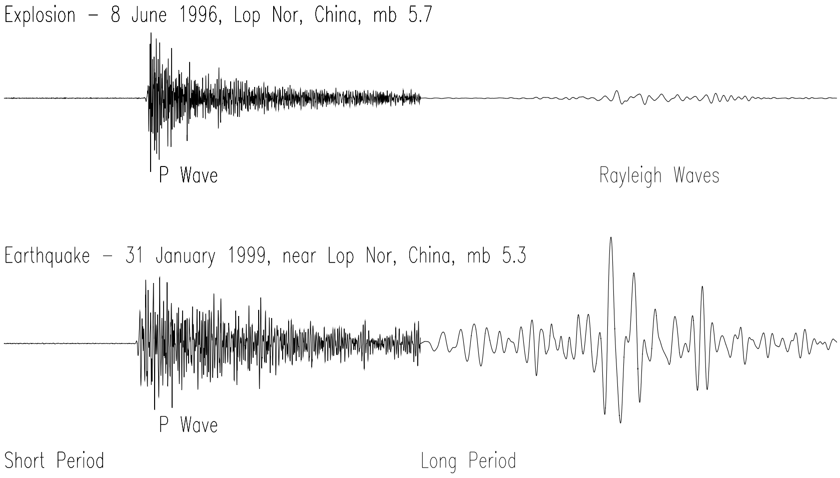


**Figure 2: Vertical component seismograms from a nuclear test explosion at Lop Nor China and a nearby earthquake recorded at the Borovoye seismometer station in Kazakhstan. Seismograms show the short-period *P* (body) waves (0.5–3.0Hz) and the long period (0.02–0.1Hz) Rayleigh (surface) waves.**

calculated for a series of known earthquake and explosion sources. Figure 3 displays body and surface wave magnitudes for 409 past underground nuclear explosions and for seismic events in 2008 which were listed in the event bulletin published by the IDC (Selby et al., 2012). Figure 3 shows that generally earthquakes and explosions populate different parts of the $m_b$:$M_S$ plot and can be separated by a screening line. Therefore, once the $m_b$ and $M_S$ of the event of interest have been calculated, its position on the $m_b$:$M_S$ plot can be used as a guide to whether the source is earthquake-like. Figure 3 shows the locations of some sources recently analysed at AWE on the $m_b$:$M_S$ plot. These include a source near to the Chinese nuclear test site at Lop Nor, and the three recent announced nuclear tests by the Democratic People's Republic of Korea (DPRK). The position of the three DPRK tests in Figure 3 close to the earthquake population highlights the need for a conservative screening line (Selby et al., 2012). A conservative screening line does however mean that some earthquake sources cannot be identified using this method (e.g. the 13th March 2003 Lop Nor earthquake).

## Source Depth Estimation

If the $m_b$:$M_S$ method fails to allow identification of a source as an earthquake, then other methods of source identification can be used. For example, if a seismic source can be shown to be deeper than a few kilometers, it can be identified as an earthquake. This is because underground explosions are unlikely to be fired at depths of more than a few kilometers. Although many methods for the estimation of source depth exist, accurate determination of depth is still a challenge for many small-to-medium sized ($m_b$4.0 to $m_b$5.5) seismic sources. Developing new and improved methods of seismic source depth estimation has therefore been a focus of the research programme at AWE Blacknest in recent years.

One of the most reliable means of estimating earthquake source depths is to identify the depth phases *pP* and *sP* on body wave seismograms recorded at long range. Once a wavespeed structure for the source region is assumed, the difference in arrival time between *P* and the depth phases can be used to estimate depth (Figure 4(a) shows the source region ray paths of *P*, *pP* and *sP*). Ideally the seismograms should have a good signal-to-noise-ratio (SNR) with *P*, *pP* and *sP* being the dominant phases on the seismograms, however often teleseismic body wave seismograms are complex and the depth phases are difficult to identify, and hence depths are difficult to estimate. Recent research at AWE Blacknest has looked at developing improved methods of identifying the depth phases *pP* and *sP*. One way to do this is to use the *F* statistic to detect seismic signals which are correlated at seismometer array stations. As shown in Figure 4(b), the computed *F* statistic trace can be used to help identify signals on the seismogram that might not otherwise have been picked by an analyst. Using standard Earth models, the 7 sec time difference between *P* and the depth phase *pP* in Figure 4(b) suggests a source depth of around 23 km. This approach to depth estimation, described in detail in Heyburn and Bowers (2008), can be applied automatically to estimate earthquake source depths using data from the global network of seismometer arrays.

Surface wave data can also be used to estimate earthquake source depths. For example, the shape of intermediate-period (40–15 sec) surface wave amplitude spectra are sensitive to the source depth. This can be exploited by computing synthetic surface wave amplitude spectra for a range of source depths and mechanisms and comparing them with the observed data to identify a best-fitting source depth and mechanism. Until recently these waves have typically been excluded from source studies as their propagation

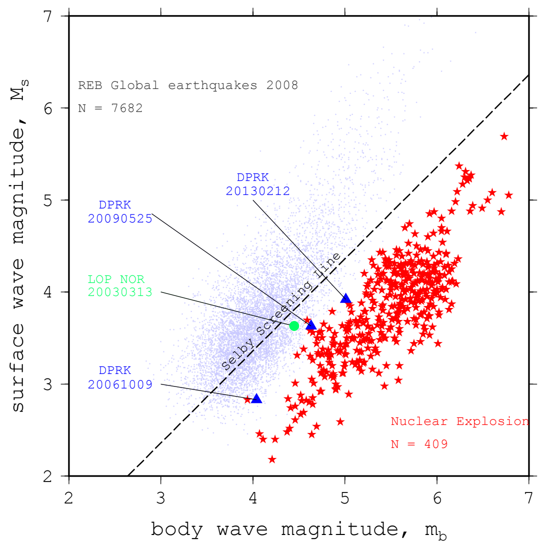


**Figure 3: $m_b$:$M_s$ plot showing the 2008 IDC global event population and the $m_b$:$M_s$ values for explosions calculated by Selby et al. (2012). The three North Korea (DPRK) explosions are indicated along with an earthquake located close to the Chinese nuclear test site at Lop Nor. The dashed line is the $m_b$:$M_s$ screening line proposed by Selby et al. (2012) now used by the IDC in Vienna. Sources that plot above this screening line can be identified as earthquakes.**

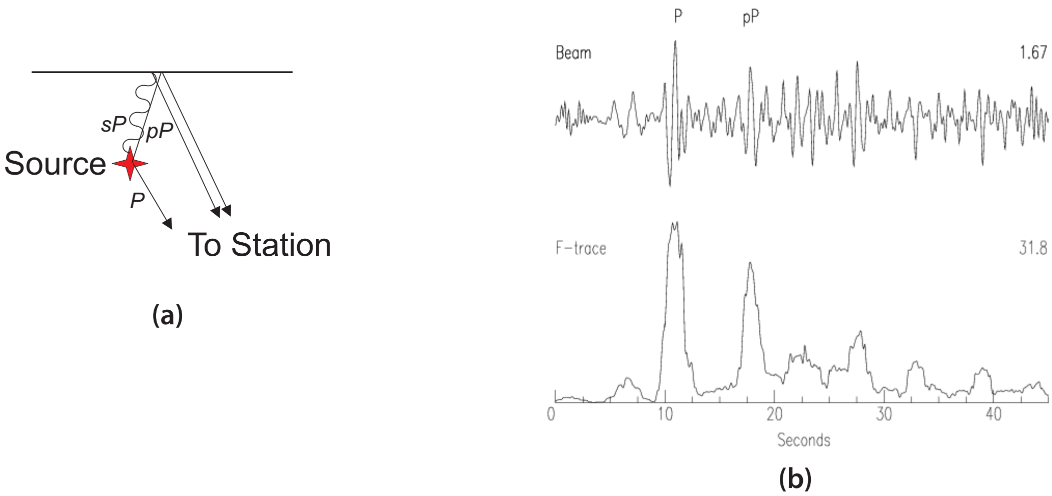


**Figure 4: (a) Ray paths of *P* and the depth phases *pP* and *sP* in the source region. (b) Seismogram and *F* statistic trace from a Lop Nor earthquake in China recorded at Yellowknife, Canada. The phases identified as *P* and *pP* with the help of the *F* statistic trace are labelled.**

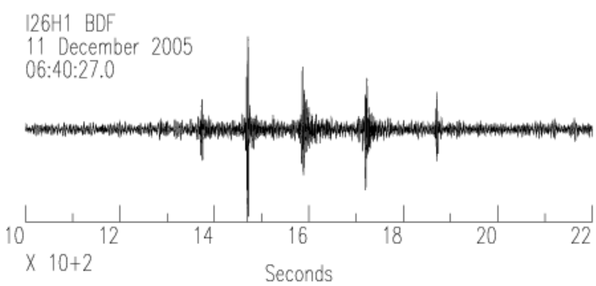


**Figure 5: Signals recorded at infrasound station I26GE in Germany from the 11th December 2005 Buncefield fuel depot explosion. The multiple arrivals associated with refracted waves on the troposphere can clearly be observed.**

characteristics were poorly predicted by the available upper mantle and crustal velocity models. However the availability of 3-D global crust and upper mantle velocity models, produced using periods as short as 16 sec, allows higher frequencies to be used with more confidence. Accurate estimates of source parameters can therefore be obtained for lower magnitude events than using conventional procedures. Fox et al. (2012) demonstrated how this approach can be used to estimate source depths and mechanisms for small to moderate sized ($4.3 \leq M_w \leq 6.4$) earthquakes across a variety of tectonic locations.

### Source Mechanism Estimation

Accurate estimates of seismic source mechanisms are another useful way of discriminating between earthquake and explosion sources. If an estimate of the source mechanism can be obtained and it is shown that the recorded signals are consistent with those predicted for an earthquake source mechanism, then the seismic source can be identified as an earthquake and the possibility of a suspicious explosion ruled out. Often the seismic sources of interest to forensic seismologists are located in regions where there are no dense local networks of seismometers. Given the magnitude of the seismic sources of interest to forensic seismologists (typically $m_b$3.5 to $m_b$6.0), source parameters often need to be estimated using a limited amount of data with good SNRs, sometimes consisting of just a few stations recording surface waves at regional distances and body waves at teleseisimc distances.

Recent research at AWE Blacknest has therefore attempted to develop methods which focus on making the most of the available data by jointly inverting body and surface wave observations to estimate the source mechanism. To do this, data from teleseismic body wave observations, three-component broadband waveform data recorded at near-regional distance stations, and surface wave amplitude spectra are inverted individually for the source mechanism. The results of these individual inversions are then evaluated in the space of the misfit functions. Ideally, the preferred focal mechanism would be the same for each individual inversion. However in reality, errors in the model parameters used, for example, the Earth model and source-time function, mean that each individual inversion has a different solution. Heyburn and Fox (2010) have showed how a multi-objective optimisation approach can be used to solve these problems and estimate source mechanisms that are consistent with multiple data sets. The advantage of this approach is that using multiple data types increases the constraint and confidence of estimated source mechanisms for sources where only a limited amount of data with good SNRs are available.

## Monitoring the CTBT using Infrasound and Hydroacoustic Data

As well as seismometer stations the IMS also has a network of infrasound and hydroacoustic stations to detect both infrasound (low frequency acoustic waves below the sensitivity range of the human ear) in the atmosphere and hydroacoustic waves in the oceans that might be generated by a nuclear test explosion. Both infrasound and hydroacoustic arrivals are now recorded in the event bulletins published by the IDC in Vienna. In recent years the group at AWE Blacknest has therefore continued to develop its expertise in analysing these different data types.

### Infrasound

Infrasound data can be use to both detect and locate nuclear test explosions in the atmosphere. Much of the energy released by an atmospheric explosion is released into the atmosphere and can propagate over large distances at high altitudes. For example, in a recent study at AWE Blacknest, acoustic waves from the 11th December 2005 Buncefield fuel depot explosion in the UK were detected at both infrasound stations and seismometer stations (air-to-ground coupled waves) at ranges of up to 1400 km across Central Europe (Ceranna et al., 2009). The propagation paths of infrasound waves are strongly affected by the horizontal wind and temperature structure of the atmosphere. Obviously this structure varies with time due to changing meteorological conditions. Ceranna et al. (2009) showed that significant improvements could be made in identifying infrasound phases using 3-D modelling and accurate models of the Earths atmosphere. For example the multiple arrivals associated with refracted waves on the troposphere observed at IMS infrasound station I26GE in Germany (Figure 5) could be predicted using this 3-D modelling.

### Hydroacoustic Data

Hydroacoustic signals can be generated by both earthquake and explosion sources. Hydroacoustic stations utilise the efficient propagation of waves in a low velocity layer in the ocean which is at approximately 1 km depth. In this channel, referred to as the sound fixing and ranging (SOFAR) channel, hydroacoustic waves are trapped and can be detected by a global network of just 11 IMS hydroacoustic stations. This network of hydroacoustic stations consists of both underwater hydrophone stations and T-phase stations. T-phase stations, which are typically located on oceanic islands, detect hydroacoustic waves which convert to seismic waves at a steep land-ocean boundary. One of the principal advantages of hydroacoustic monitoring is the low detection threshold (thresholds are generally less than 0.001 kt TNT in the open ocean) of the 11 station network that is a result of the efficient propagation of waves in the SOFAR channel.

As well as detecting and locating sources, hydroacoustic data can also be used to discriminate between an explosion in the water and naturally occurring seismic sources such as earthquakes which sometimes generate seismic waves which convert to hydroacoustic waves. For example,

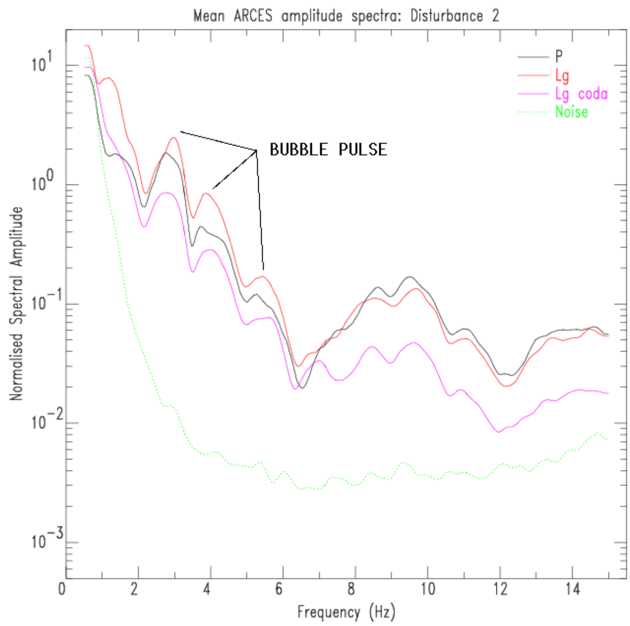


**Figure 6: Amplitude spectra of waves recorded at ARCES (Norway) from the 12th August 2000 Kursk submarine disaster. The presence of spectral scalloping in the signal (the bubble pulse) is evidence of an underwater explosion source.**

the oscillation in size of bubbles generated by an underwater explosion causes scalloping in the observed amplitude spectra of the hydroacoustic waves (Figure 6). This bubble pulse was clearly observed for signals recorded on IMS stations from the 12th August 2000 Kursk submarine disaster and allowed the source of the observed signals to be identified as an explosion source.

## Conclusions

For the last 50 years AWE Blacknest has provided the UK government with seismological advice on the monitoring of nuclear test explosions. The research program at Blacknest not only ensures the credibility of this advice, but also provides the tools for effective event analyses (e.g. the recent announced North Korea nuclear test explosions). Some of the recent research carried out at Blacknest has focused on further improving the methods that are used to discriminate between the seismic signals generated by earthquakes and those generated by explosions. This has included revisiting the $m_b$ and $M_S$ method of earthquake source identification, and developing improved methods of estimating seismic source parameters. Often the methods developed at AWE Blacknest have applications in earthquake seismology. For example, work on seismic source parameter estimation could prove useful in tectonic studies. Going forward, the group at AWE Blacknest continue to work on improving the methods used to analyse waveform data from the IMS network.

## References

Ceranna, L., Le Pichon, A., Green, D. N., & Mialle, P. (2009). The Buncefield explosion: A benchmark for infrasound analysis across Central Europe. *Geophys. J. Int.*, **177:** 491–508.

Fox, B. D., Selby, N. D., Heyburn, R., & Woodhouse, J. H. (2012). Shallow seismic source parameter determination using intermediate-period surface wave amplitude spectra. *Geophys. J. Int.*, **191:** 601–615.

Heyburn, R., & Bowers D. (2008). Earthquake depth determination using the *F* trace and associated probability. *Bull. Seismol. Soc. Am.*, **98:** 18–35.

Heyburn, R., & Fox, B. (2010). Multi-objective analysis of body and surface waves from the Market Rasen (UK) earthquake. *Geophys. J. Int.*, **181:** 532–544.

Heyburn, R., Selby, N. D., & Fox, B. D. (2013). Estimating earthquake source depths by combining surface wave amplitude spectra and teleseismic depth phase observations. *Geophys. J. Int.*, **194:** 1000–1010.

Liebermann, R. C., & Pomeroy, P. W. (1967). Excitation of surface waves by events in southern Algeria. *Science*, **156:** 1098–1100.

Nippress, A., Green, D. N., Marcillo, O. E., & Arrowsmith, S. J. (2014). Generating regional infrasound celerity-range models using ground-truth information and the implications for event location. *In press.*

Selby, N. D., Marshall, P. D., & Bowers, D. (2012). $m_b$:$M_S$ event screening revisited. *Bull. Seismol. Soc. Am.*, **102:** 88–97.

Selby, N. D. (2013). A multiple-filter *F* detector method for signal detection at medium-aperture arrays. *Geophys. J. Int.*, **192:** 1189–1195.

# Three Time-Scales of Performance-Based Earthquake Engineering

**Iunio Iervolino**
*Associate Professor*
*Dipartimento di Strutture per l'Ingegneria e l'Architettura*
*Università degli Studi di Napoli Federico II, Naples, Italy*

Recent earthquake engineering research is focusing on three time scales of seismic risk, which may be defined as:

(i) real-time, that is during the event;

(ii) near-real-time, that is in the aftershock sequence to a major earthquake;

(iii) long-term life-cycle of degrading structures.

Each of these presents challenges and issues, which require development of specific tools for risk management. In the following, a few results in this direction, as presented in the recent SECED talk of the author, are briefly summarised. All the models are reconcilable, meaning that they represent time-scale-specific declensions of the performance-based earthquake engineering approach.

(i) The tool to manage seismic risk in real-time is earthquake early warning (EEW). The basic elements of an EEW system are: a network of seismic instruments, a processing unit for the data measured by the sensors, and a transmission infrastructure spreading the alarm to the end users. This alarm may trigger security actions, manned or automated, expected to reduce the seismic risk in real-time (Figure 1).

So far, reasonably, most of the research in this field has been led by seismologists, as the issues to determine essential feasibility of EEW were mainly related to the earthquake source. Many of them have been brilliantly solved, and the principles of this discipline are collected in the so-called "real-time seismology". On the other hand, to date, comparatively little attention has been given to EEW in earthquake engineering, and design approaches for structure-specific EEW are mostly lacking, although the topic is certainly worthwhile to pursue.

The key design points for EEW applied to a specific structure are: (a) the estimated earthquake potential on the basis of the EEW information; (b) the available time before the earthquake strikes, or lead-time; and (c) the system performance (proxy for the loss) associated to the case the alarm is issued. These issues are collectively identified as a possible performance-based approach to the design of structure-specific EEW.

For more information on this work, refer to Iervolino (2011).

(ii) Major earthquakes (i.e., mainshocks) typically trigger a sequence of lower-magnitude events clustered both in time and space. Recent advances in seismic hazard analysis model aftershock occurrence (given the main event) as a stochastic process with rate that decays with time as a negative power law.

Short-term risk assessment, that is at the time-scale of weeks/months around a major event, is gathering increasing research attention due to the compelling need for decision makers to have the quantitative tools that enable the

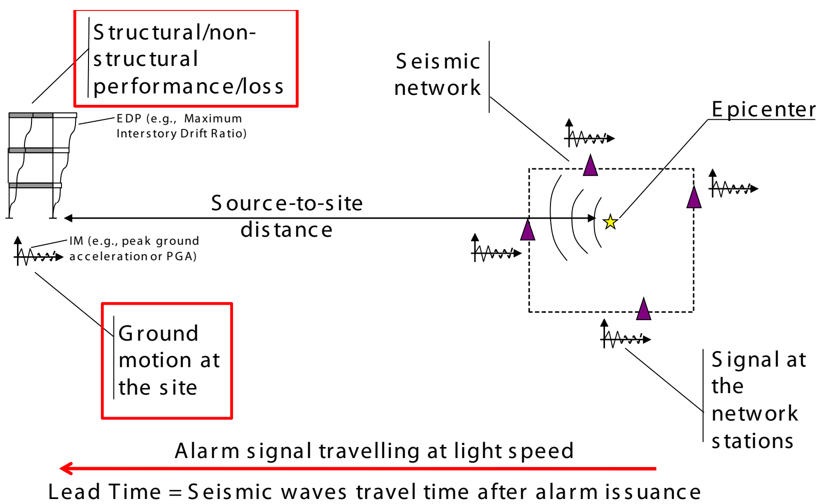


**Figure 1: Sketch of regional EEW systems for the real-time risk management of specific structures.**

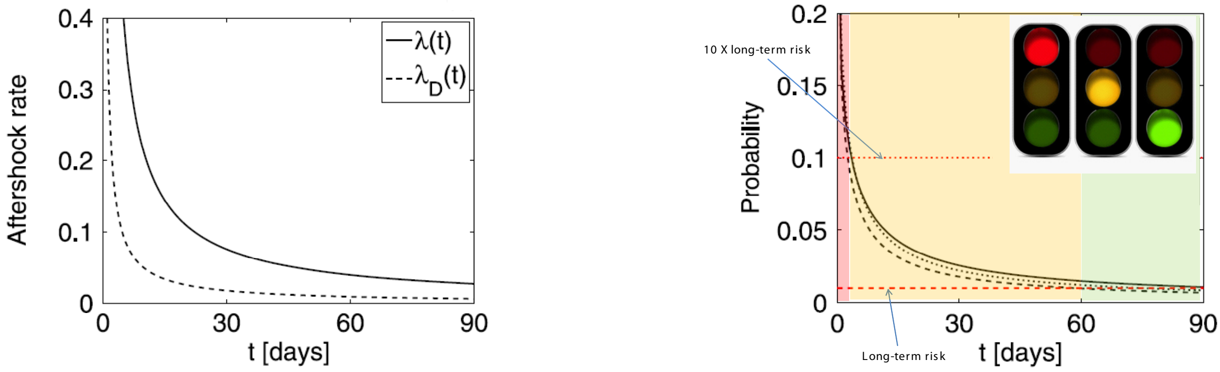


**Figure 2: Example of decay rate of aftershock and damaging aftershocks (subscript 'D') to a structure within 90 days after the mainshock (left). Weekly failure probability for a structure damaged in the mainshock and tagging criteria based on conventional risk thresholds (right).**

management of such a risk.

In fact, because the structural systems of interest might have suffered some damage in the mainshock, possibly worsened by damaging aftershocks, the failure risk may be large until the intensity of the sequence reduces or the structure is repaired. Of particular interest is the evaluation of the failure probability for mainshock-damaged structures exposed to the following aftershock sequence. This may be referred to as building tagging and allows the monitoring of the variation of structural risk due to both increased vulnerability, caused by cumulative damage, and time-decaying aftershock hazard, and to decide whether: to prohibit access to anyone (i.e., red tag); allow access only to trained agents for emergency operations (i.e., yellow tag); or to halt business interruptions allowing normal occupancy (i.e., green tag) (Figure 2).

On the basis of age-dependent stochastic processes, it is possible to derive closed-form approximations for the aftershock reliability of simple damage-cumulating structures, conditional on different information about the structure. The developed models may represent a basis for handy tools aimed at risk-informed tagging by stakeholders and decision makers.

For more information on this work, refer to Iervolino et al. (2013a).

(iii) Life-cycle analysis of structures requires stochastic modelling of deterioration. The categories of degradation phenomena typical of structures are progressive degradation of structural characteristics and cumulative damage due to point overloads; i.e., earthquake clusters. Ageing, which in some cases may show an effect in increasing seismic structural fragility, is often related to an aggressive environment which worsens mechanical features of structural elements. To be able to predict the evolution of this kind of wear is especially important in design of maintenance policies. Shocks from earthquake clusters potentially accumulate damage on the hit structure during its lifetime, unless partial or total restoration is carried out; i.e., within a cycle. If both deterioration effects may be measured in terms of the same parameter expressing the structural capacity, for example the residual ductility to collapse, then the total wear may be susceptible of the representation as a function

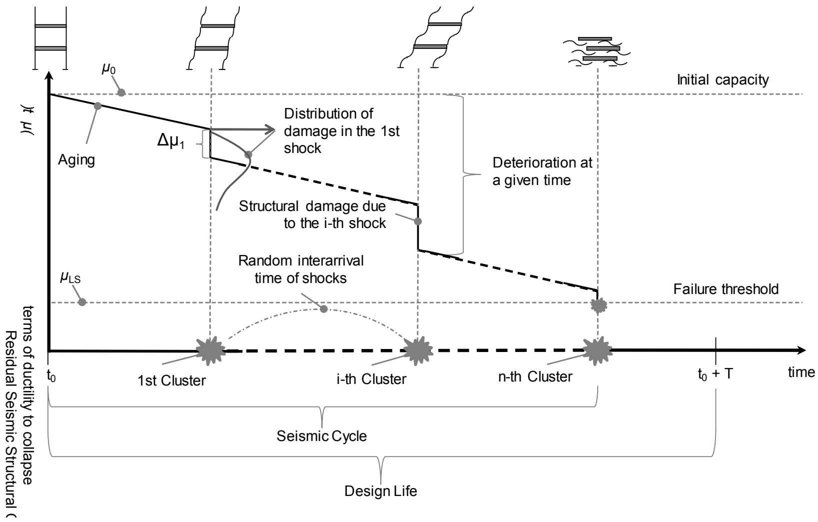


**Figure 3: Seismic cycle representation for a structure subjected to aging and repeated earthquake shocks, when degradation affects residual capacity to failure.**

of time in Figure 3, where a conventional threshold corresponding to a limit-state of interest is also depicted.

Closed-form approximations, for life-cycle structural assessment, may be obtained in terms of absolute failure probability, as well as conditional on different knowledge about the structural damage history. Moreover, under some assumptions, it is possible to express total degradation (i.e., due to both ageing and shocks) in simple forms, amenable to numerical solution. Finally, the possible transformation of the repeated-shock effect due to earthquakes in an equivalent ageing may be derived.

To be able to get closed-form approximation of the reliability of deteriorating structures may help simple life-cycle assessment with respect to traditional simulation-based procedures employed in the context of performance-based earthquake engineering.

For more information on this work, refer to Iervolino et al. (2013b).

## References


Iervolino I., (2011). Performance-based earthquake early warning. *Soil Dynamics and Earthquake Engineering.* **31:** 209–222.

Iervolino I., Giorgio M., & Chioccarelli E., (2013a). Closed-form aftershock reliability of damage-cumulating elastic-perfectly-plastic systems. *Earthquake Engineering and Structural Dynamics*, **43:** 613–615.

Iervolino I., Giorgio M., & Chioccarelli E., (2013b). Gamma degradation model for earthquake-resistant structures. *Structural Safety*, **45:** 48–58.


# Seismic Design Requirements in Building Regulations for England

In the UK, Seismic Design has not traditionally been required to meet the Building Regulations. However, this requirement was introduced from 1st October 2013, when Part A of the Building Regulations in England was amended to include the following at the end of Section 5 (Disproportionate Collapse):

> *5.5 Seismic Design is not usually required for buildings classified by Table 11 as being in Consequence Classes 1, 2a and 2b. For buildings classified as Consequence Class 3 [High Hazed facilities] the risk assessment should consider if there is any need to carry out seismic design, although such a need is not an explicit requirement for these buildings.*

In addition, BS EN 1998 “Design of Structures for Earthquake Resistance” [Eurocode 8] was added as a deemed-to-satisfy reference.

Further information on this change may be found on the Department for Communities and Local Government web site, www.communities.gov.uk.

The requirements for Scotland, Wales, and Northern Ireland are expected to follow, and the appropriate regional government web site should be consulted for the current position.

*This summary provided by Paul Doyle.*

# Forthcoming Events

| Date | Venue | Title | People |
|---|---|---|---|
| 30/4/2014 at 18:00 | Institution of Civil Engineers, 1 Great George St, London | *The REDi™ Rating System: A Framework for Resilience-based Earthquake Design* | *Speaker*: **Ibrahim Almufti** (Arup, San Francisco) *Organiser*: **Damian Grant** (Arup) |
| 28/5/2014 | Institution of Civil Engineers, 1 Great George St, London | *Dynamic Response of Anchorage in Concrete* | *Speakers*: **Rolf Eligehausen** (Universität Stuttgart) *Organisers*: **Ian Smith** (Atkins) |
| 24/9/2014 at 18:00 | Institution of Civil Engineers, 1 Great George St, London | *Current Trends in the Seismic Design and Analysis of Bridges* | *Speaker*: **Andreas Kappos** (City University) *Organiser*: **Ahmed Elghazouli** (Imperial College) |

For up-to-date details of SECED events, visit the website: **www.seced.org.uk**

# SECED 2015 Conference: Earthquake and Civil Engineering Dynamics for Risk, Mitigation and Recovery

SECED 2015 is a 2-day conference on Earthquake and Civil Engineering Dynamics taking place on 9–10 July 2015 at Homerton College, Cambridge. This will be the first major conference to be held in the UK on this topic since SECED hosted the 2002 European Conference on Earthquake Engineering in London. The programme will provide an opportunity for both researchers and practitioners to share the latest knowledge and techniques for understanding the dynamic behaviour of structures, of earthquakes and of their effects on the natural and built environment. The conference will bring together experts from a broad range of disciplines, including structural engineering, nuclear engineering, seismology, geology, geophysics, geotechnical engineering, urban development, social sciences, business and insurance; all focused on risk, mitigation and recovery.

Further announcements will be made through the SECED membership mailing list, the SECED website and newsletter.

**Conference themes** will be:

- Risk and Catastrophe Modelling
- Geotechnical Earthquake Engineering
- Seismic Design for Nuclear Facilities
- Masonry and Non-engineered Structures
- Fracking and Induced Seismicity
- Vibrations, Blast and Civil Engineering Dynamics
- Seismic Assessment and Retrofit of Engineered and Non-Engineered Structures
- Innovations in Seismic Design
- Dams and Hydropower
- Seismic Hazard and Engineering Seismology
- Social Impacts and Community Recovery

**Keynote speakers** will include:
Don Anderson (CH2M HILL, Seattle), Andrew Whittaker (University at Buffalo) and Tiziana Rossetto (University College London), and others to be announced.

**Cambridge, UK (© Robert Massam)**

## SECED

SECED, The Society for Earthquake and Civil Engineering Dynamics, is the UK national section of the International and European Associations for Earthquake Engineering and is an affiliated society of the Institution of Civil Engineers. It is also sponsored by the Institution of Mechanical Engineers, the Institution of Structural Engineers, and the Geological Society. The Society is also closely associated with the UK Earthquake Engineering Field Investigation Team. The objective of the Society is to promote co-operation in the advancement of knowledge in the fields of earthquake engineering and civil engineering dynamics including blast, impact and other vibration problems.

For further information please contact the SECED Secretary at the ICE at: secretary@seced.org.uk.

For contributions to the newsletter, please contact the Editor, Damian Grant, for further details: damian.grant@arup.com.

# Notable Earthquakes March 2013 – June 2013

## Reported by British Geological Survey

**Issued by: Davie Galloway, British Geological Survey, July 2013 and January 2014.**
**Non British Earthquake Data supplied by The United States Geological Survey.**

| | | | Time | | | Dep | Magnitude | | | |
|---|---|---|---|---|---|---|---|---|---|---|
| Year | Day | Mon | UTC | Lat | Lon | km | ML | Mb | Mw | Location |
| 2013 | 01 | MAR | 12:53 | 50.90N | 157.45E | 33 | | | 6.4 | KURIL ISLANDS |
| 2013 | 01 | MAR | 13:20 | 50.96N | 157.41E | 29 | | | 6.5 | KURIL ISLANDS |
| 2013 | 03 | MAR | 05:41 | 25.98N | 99.81E | 8 | | | 5.2 | YUNNAN, CHINA |
| Thirty people injured, three seriously, 700 homes collapsed and over 2,500 homes damaged in the epicentral area. | | | | | | | | | | |
| 2013 | 04 | MAR | 03:26 | 64.51N | 4.21W | 10 | 3.5 | | | NORWEGIAN SEA |
| 2013 | 06 | MAR | 13:16 | 48.41N | 4.10W | 5 | 2.2 | | | NORTHWEST FRANCE |
| 2013 | 10 | MAR | 21:18 | 57.00N | 5.79W | 8 | 1.8 | | | MALLAIG, HIGHLAND |
| Felt Mallaig (2 EMS). | | | | | | | | | | |
| 2013 | 10 | MAR | 22:51 | 6.60S | 148.17E | 28 | | | 6.5 | PAPUA NEW GUINEA |
| 2013 | 15 | MAR | 10:43 | 57.01N | 1.97E | 14 | 3.1 | | | CENTRAL NORTH SEA |
| 2013 | 16 | MAR | 07:03 | 52.54N | 0.79E | 5 | 2.1 | | | WATTON, NORFOLK |
| 2013 | 21 | MAR | 04:13 | 54.54N | 2.88W | 3 | 1.2 | | | GLENRIDDING, CUMBRIA |
| Felt Glenridding (2 EMS). | | | | | | | | | | |
| 2013 | 22 | MAR | 10:32 | 61.58N | 4.47E | 15 | 3.7 | | | NORWEGIAN COAST |
| 2013 | 22 | MAR | 12:57 | 52.97N | 4.46W | 13 | 2.2 | | | LLEYN PENINSULA |
| 2013 | 22 | MAR | 13:52 | 61.62N | 4.47E | 6 | 3.5 | | | NORWEGIAN COAST |
| 2013 | 24 | MAR | 22:02 | 57.72N | 5.55W | 8 | 2.0 | | | LOCH MAREE, HIGHLAND |
| Felt Gairloch and Poolewe (3 EMS). | | | | | | | | | | |
| 2013 | 27 | MAR | 02:03 | 23.83N | 121.22E | 19 | | | 5.9 | TAIWAN |
| One person killed, 86 injured and several buildings damaged in Nantou. | | | | | | | | | | |
| 2013 | 06 | APR | 04:42 | 3.52S | 138.48E | 66 | | | 7.0 | PAPUA, INDONESIA |
| 2013 | 09 | APR | 11:52 | 28.43N | 51.59E | 12 | | | 6.4 | SOUTHERN IRAN |
| At least 37 people killed, 850 injured and over 700 houses damaged or destroyed in the epicentral area. | | | | | | | | | | |
| 2013 | 14 | APR | 01:32 | 6.48S | 154.61E | 31 | | | 6.6 | PAPUA NEW GUINEA |
| 2013 | 16 | APR | 10:44 | 28.03N | 62.00E | 80 | | | 7.7 | IRAN/PAKISTAN BORDER |
| At least 40 people killed, 300 injured and some 35,000 made homeless in the Mashkel area, Pakistan. A further 27 people reported injured in south-eastern Iran. | | | | | | | | | | |
| 2013 | 16 | APR | 22:55 | 3.21S | 142.54E | 13 | | | 6.6 | PAPUA NEW GUINEA |
| 2013 | 19 | APR | 03:05 | 46.22N | 150.79E | 110 | | | 7.2 | KURIL ISLANDS |
| A small tsunami was observed on Shakotan, Hokkaido, Japan. | | | | | | | | | | |
| 2013 | 20 | APR | 00:02 | 30.31N | 102.89E | 14 | | | 6.6 | WESTERN SICHUAN, CHINA |
| At least 196 people killed, another 11,500 injured and 21 still reported as missing, presumed dead. Many houses and roads were destroyed or damaged, communications were disrupted and several power outages occurred in the area. | | | | | | | | | | |
| 2013 | 23 | APR | 23:14 | 3.90S | 152.13E | 10 | | | 6.5 | PAPUA NEW GUINEA |
| 2013 | 24 | APR | 09:25 | 34.53N | 70.22E | 64 | | | 5.5 | HINDU KUSH, AFGHANISTAN |
| Eighteen people killed, 141 injured and over 670 houses damaged in the Jalalabad/Mehtar Lam region of Afghanistan. | | | | | | | | | | |

| | | | Time | | | Dep | Magnitude | | | |
|---|---|---|---|---|---|---|---|---|---|---|
| Year | Day | Mon | UTC | Lat | Lon | km | ML | Mb | Mw | Location |
| 2013 | 05 | MAY | 16:07 | 50.39N | 4.62W | 5 | 1.8 | | | LOSTWITHIEL, CORNWALL |
| Felt Par and St Neot (2 EMS). | | | | | | | | | | |
| 2013 | 11 | MAY | 02:08 | 26.56N | 57.77E | 15 | | | 6.1 | SOUTHERN IRAN |
| Two people killed, 20 injured and many buildings destroyed in the epicentral region. | | | | | | | | | | |
| 2013 | 14 | MAY | 00:32 | 18.73N | 145.29E | 602 | | | 6.8 | NORTHERN MARIANA ISLANDS |
| 2013 | 15 | MAY | 17:43 | 57.67N | 5.58W | 8 | 2.8 | | | GAIRLOCH, HIGHLAND |
| Felt Gairloch, Charlestown, Midtown, North Erradale, South Erradale, Strath, Badachro and Poolewe, Higland (3 EMS). | | | | | | | | | | |
| 2013 | 18 | MAY | 19:18 | 56.78N | 5.71W | 10 | 2.9 | | | ACHARACLE, HIGHLAND |
| Felt Acharacle, Strontian, Kilchoan, Glenfinnan and the Isle of Lismore (3 EMS). | | | | | | | | | | |
| 2013 | 23 | MAY | 17:19 | 23.01S | 177.23W | 174 | | | 7.4 | TONGA |
| 2013 | 24 | MAY | 05:44 | 54.89N | 153.22E | 598 | | | 8.3 | SEA OF OKHOTSK |
| 2013 | 24 | MAY | 14:56 | 52.24N | 151.44E | 624 | | | 6.7 | SEA OF OKHOTSK |
| 2013 | 29 | MAY | 03:16 | 52.88N | 4.72W | 11 | 3.8 | | | LLEYN PENINSULA, GWYNEDD |
| Felt widely across North Wales and as far away as the Isle of Man (140 km to the north), Southport (140 km to the north-east) and Ireland (110 km to the west) (4 EMS). | | | | | | | | | | |
| 2013 | 29 | MAY | 03:20 | 52.88N | 4.71W | 10 | 1.7 | | | LLEYN PENINSULA, GWYNEDD |
| Felt Bryncroes and Aberdaron, Gwynedd (2 EMS). | | | | | | | | | | |
| 2013 | 29 | MAY | 17:49 | 57.58N | 5.43W | 3 | 1.5 | | | TORRIDON, HIGHLAND |
| 2013 | 30 | MAY | 22:06 | 52.89N | 4.73W | 11 | 0.8 | | | LLEYN PENINSULA, GWYNEDD |
| Felt Bryncroes and Aberdaron, Gwynedd (2 EMS). | | | | | | | | | | |
| 2013 | 31 | MAY | 06:22 | 52.88N | 4.71W | 10 | 1.4 | | | LLEYN PENINSULA, GWYNEDD |
| Felt Bryncroes and Aberdaron, Gwynedd (2 EMS). | | | | | | | | | | |
| 2013 | 02 | JUN | 02:56 | 56.12N | 6.13W | 8 | 1.5 | | | COLONSAY, ARGYLL & BUTE |
| Felt Scalasaig, Colonsay (2 EMS). | | | | | | | | | | |
| 2013 | 02 | JUN | 05:43 | 23.79N | 121.14E | 17 | | | 6.2 | TAIWAN |
| Four people killed (three by landslides), 21 injured and around 100 buildings damaged in Nantou and Taichung. | | | | | | | | | | |
| 2013 | 10 | JUN | 03:12 | 59.93N | 0.20E | 8 | 2.0 | | | NORTHERN NORTH SEA |
| 2013 | 10 | JUN | 03:13 | 59.93N | 0.20E | 8 | 1.6 | | | NORTHERN NORTH SEA |
| 2013 | 13 | JUN | 16:47 | 10.00S | 107.24E | 9 | | | 6.7 | SOUTH OF JAVA, INDONESIA |
| 2013 | 15 | JUN | 17:34 | 11.76N | 86.93W | 30 | | | 6.5 | NICARAGUA |
| 2013 | 23 | JUN | 12:08 | 56.01N | 6.07W | 9 | 1.8 | | | FIRTH OF LORN, HIGHLAND |
| 2013 | 24 | JUN | 22:04 | 10.70N | 42.59W | 10 | | | 6.6 | NORTHERN MID-ATLANTIC RIDGE |
| 2013 | 26 | JUN | 03:51 | 53.53N | 1.01W | 1 | 1.9 | | | DONCASTER, S YORKSHIRE |
| Felt Fosterhouse (2 EMS). | | | | | | | | | | |
| 2013 | 26 | JUN | 22:28 | 52.88N | 4.72W | 9 | 2.8 | | | LLEYN PENINSULA, GWYNEDD |
| Origin time: 22:28:01s UTC. Felt throughout north Gwynedd in Pwllheli, Caernarfon, Bangor, Menai Bridge, Blaenae Ffestiniog, Bodorgan and Holyhead (3 EMS). | | | | | | | | | | |
| 2013 | 26 | JUN | 22:28 | 52.88N | 4.70W | 8 | 2.4 | | | LLEYN PENINSULA, GWYNEDD |
| Origin time: 22:28:29s UTC. Felt throughout north Gwynedd in Pwllheli, Caernarfon, Bangor, Menai Bridge, Blaenae Ffestiniog, Bodorgan and Holyhead (3 EMS). | | | | | | | | | | |
| 2013 | 26 | JUN | 22:30 | 52.88N | 4.71W | 8 | 1.2 | | | LLEYN PENINSULA, GWYNEDD |
| Felt Bryncroes, Gwynedd (2 EMS). | | | | | | | | | | |
| 2013 | 30 | JUN | 12:13 | 49.69N | 4.56W | 8 | 1.8 | | | ENGLISH CHANNEL |